

Fe₃O₄(001) films on Fe(001) - termination and reconstruction of iron rich surfaces

N. Spiridis,¹ J. Barbasz,¹ Z. Łodziana,^{2,3} and J. Korecki^{1,4}

¹Institute of Catalysis & Surface Chemistry, Polish Academy of Sciences, Kraków, Poland,

²Center for Atomic-scale Materials Physics, DTU, Lyngby, Denmark,

³ Henryk Niewodniczański Institute of Nuclear Physics, Polish Academy of Sciences, Kraków, Poland,

⁴Faculty of Physics & Applied Computer Science, AGH University of Science and Technology, Kraków, Poland.

High-quality and impurity-free magnetite surfaces with $(\sqrt{2}\times\sqrt{2})R45^\circ$ reconstruction have been obtained for the Fe₃O₄(001) epitaxial films deposited on Fe(001). Based on atomically resolved STM images for both negative and positive sample polarization and Density Functional Theory calculations, a consistent model of the magnetite (001) surface terminated with Fe ions forming dimers on the reconstructed $(\sqrt{2}\times\sqrt{2})R45^\circ$ octahedral iron layer is proposed.

68.47.Gh, 68.37.Ef, 68.55.-a

Controversies about structural details of the Fe₃O₄(001) polar surface,¹ constituting one of the possible low-index magnetite terminations, remain unsolved since the very first scanning tunneling microscopy (STM) experiment on this surface.² Magnetite (Fe₃O₄) crystallizes in the inverse spinel structure with a lattice constant of 8.40 Å. Fe ions are located at two different interstitial sites octahedrally and tetrahedrally coordinated to oxygen that forms a close-packed cubic structure. The tetrahedral sites (A) are occupied by trivalent Fe ions, whereas a randomly arranged mixture of the tri- and divalent Fe ions occupies the octahedral sites (B). At T~125 K, magnetite undergoes a metal-insulator transition, known as the Verwey transition and commonly interpreted as a long-range electron charge ordering in the octahedral Fe sublattice. For a review of magnetite properties see Refs. 3, 4.

The structure of the (001) magnetite surface has been intensively studied for single crystals^{2, 5, 6, 7, 8} as well as for epitaxial films.^{9, 10, 11, 12, 13, 14, 15} The surface is usually discussed as being composed of atomic sublayers, containing either only tetrahedral iron ions Fe(A) (the so-called A-layer) or oxygen and octahedral iron ions Fe(B) (the so-called B-layer). The distance between A or B layers is about 2.1 Å, whereas the smallest interlayer (A-B) spacing is about 1.1 Å. The most typical reconstruction for the (001) surface is ($\sqrt{2} \times \sqrt{2}$)R45° (corresponding to the 8.40x8.40 Å² surface mesh) as related to the (1x1) primitive surface unit cell with the 5.94x5.94 Å² periodicity of the bulk terminated surface. Neither A nor B bulk termination of the Fe₃O₄(001) surface is charge-compensated, and a number of models assume that the charge neutrality condition is a driving force behind the reconstruction. The obvious way to achieve the autocompensated Fe₃O₄(001) surface with the observed reconstruction is to remove certain surface atoms: half of Fe³⁺ ions for the A termination^{10, 11, 12, 14} or a number of oxygens for the B termination^{10, 13}. However, surface stability can be achieved also through electronic degrees of freedom. Thus, models with full A- or B-type layer termination with a specific surface electronic and geometric structure were also proposed.^{2, 5, 7, 8, 9} The interpretation was obscured by ambiguity of the surface stoichiometry since there were no procedures to control whether the surface layer was oxygen- or iron-rich. Both single crystal and epitaxial film surfaces for Ultra High Vacuum (UHV) studies are prepared in processes occurring in a broad range of temperature and oxygen partial pressures. Consequently, there is no consistency between the variety of the proposed models and the real space images of the Fe₃O₄(001) surfaces obtained by STM.^{2, 5, 8, 9, 13, 15}

The reported STM images of the Fe₃O₄(001) surface differ in many details, but one feature is common for all observations. On flat terraces, which are terminated with steps of 2.1 Å in height, atomic rows spaced by 6 Å are seen at positive sample biases. These are mutually perpendicular on neighboring terraces. The step height corresponds to the A-A or B-B layer spacing. Due to symmetry and spacing of the rows, they are commonly attributed to Fe ions in octahedral sites. The occupied state images are rarely reported. They reveal elongated shapes forming a square 8.4 Åx8.4 Å mesh, interpreted as clusters of atoms within the tetrahedral termination.^{5, 9} To our knowledge, images of the empty and filled states have never been observed for the same sample.

In the present study, we propose a new method of a preparing Fe₃O₄(001) surface with a

stable and reproducible $(\sqrt{2}\times\sqrt{2})R45^\circ$ reconstruction by depositing magnetite on a Fe(001) film. The surface gives STM images of high stability and atomic resolution for negative and positive sample polarization, allowing us to image details of the surface structure and, when combined with Density Functional Theory (DFT) calculations, to infer a consistent model of the surface. We show that using different preparation methods the magnetite surface with octahedral (B) or partially filled and dimeric tetrahedral (A) termination can be stabilized.

The magnetite films were obtained in a UHV system on cleaved MgO(001) substrates. Two preparation schemes were used. $\text{Fe}_3\text{O}_4(001)$ films were prepared in a „classical” way, directly on MgO, by oxygen assisted deposition of Fe at 250 °C, as described in our earlier papers.^{15,16} The new preparation method consisted of depositing a 200 Å buffer layer of epitaxial Fe(001) on the MgO(001) substrate to guarantee an iron reservoir to balance the magnetite stoichiometry. On the Fe(001) surface an oxide layer was formed by oxygen-assisted deposition of Fe at 10^{-4} Pa O_2 on the substrate, which was held at 250 °C. Finally, the samples were annealed at 500 °C for 60 minutes. The as-prepared films were characterized *in situ* by Auger electron spectroscopy and LEED, and *ex situ* by the conversion electron Mössbauer spectroscopy, and display typical $\text{Fe}_3\text{O}_4(001)$ features. The $(\sqrt{2}\times\sqrt{2})R45^\circ$ reconstruction remained stable also after the post-preparation annealing, whereas the films deposited directly on MgO(001) showed, after the same treatment, major changes of the surface structure induced by the diffusion of Mg from the substrate into the magnetite film.^{13,15} Apparently, the Fe(001) layer sets an effective barrier for Mg diffusion.

The STM measurements were carried out *in situ* with a room-temperature STM head (Burleigh) using electrochemically etched tungsten tips. The corresponding theoretical simulations were based on DFT calculations. The plane wave pseudopotential method¹⁷ with the gradient corrected exchange-correlation functional¹⁸ was used. The Monkhorst-Pack k-point sampling mesh with density of 0.1\AA^{-1} , together with a kinetic energy cutoff of 340 eV and the charge density grid of 680 eV were applied. The electronic density was determined by iterative diagonalization of the Kohn-Sham Hamiltonian, and the resulting Kohn-Sham eigenstates were populated according to the Fermi statistics with a finite temperature smearing of $kT=0.015$ eV. The calculations reproduce the magnetic and structural properties of the bulk magnetite very well, giving the lattice constant $a_0=8.39$ Å and magnetic moments of $3.34\ \mu_B$ for Fe(B) and $3.28\ \mu_B$ for Fe(A). The surface calculations were performed in a stoichiometric slab geometry with eight atomic layers in the reconstructed $(\sqrt{2}\times\sqrt{2})R45^\circ$ unit

cell. The vacuum region extended up to 16 Å and the dipole correction was applied. The STM topographs were simulated based on the Tresoff-Hamann formalism.¹⁹

Large-scale in situ STM images (not shown) for Fe₃O₄(001) surfaces prepared on Fe(001) epitaxial films reveal surface topography similar to that observed for well-ordered single crystalline Fe₃O₄(001) surfaces. Flat terraces, extending over 30x30 nm² in average, are separated by 2 Å high atomic steps along the <110> directions, terminated by a pair of screw dislocations. Atomically resolved images could be obtained in a broad range of positive and negative bias voltages. The most typical ones, appearing reproducibly for all investigated samples (over 20) are shown in Fig. 1. At the positive sample bias V_s = 0.8 V, a network of regularly arranged dark features with the 8.4x8.4 Å² periodicity corresponding to the ($\sqrt{2}\times\sqrt{2}$)R45° reconstruction is imposed on the bright rows along the <110> directions spaced by 6 Å (Fig.1a,b). The rows are mutually perpendicular on neighboring terraces. The sample bias can be reproducibly changed to negative values (typically V_s = -1.7 V), yielding entirely different images dominated by well-separated bright shapes with locally different surface densities (Fig.1c,d). The shapes, which we call ovals, are elongated in the <110> directions and form rows along the same directions, spaced by 6 Å. Distance between the ovals in a row is 12 Å. Consequently, in the densest packed areas, ovals form a 8.4x8.4 Å² mesh. The every second row of ovals is frequently missing, and thus the areas with a 12x12 Å² mesh are formed. The oval statistics over 2500 nm² taken for many terraces and samples gives the average occupation of 0.50±0.03 monolayer of ovals. The ovals, apart from their densities, are very similar to the shapes observed by Tarrach *et al.* and Gaines *et al.* for single-crystalline and thin-film surfaces, respectively. Gaines *et al.* described them as diffused clusters of atoms, which may consist of both tetrahedral and octahedral Fe ions, and are difficult to interpret due to a complicated atomic arrangement.

The exceptional stability of the STM images allowed us to change sample polarization during the scan (as shown by the arrow in Fig.1c), and thus the respective positions of atomic scale details in the pair of images could be easily identified. The determination of the absolute positions of the atomic details with respect to the (1x1) surface unit cells takes into account the fact that any row-like features appearing along <110> are due to octahedral irons. Regardless of the strong electronic effect, which is obvious from the very strong dependence of the images on the bias voltage, the position of the ovals between the octahedral iron rows suggests that they appear predominantly due to tunneling from tetrahedral Fe ions, and

consequently we assume that the surface is terminated with a partially occupied layer of the tetrahedral Fe(A) ions. The atomic images presented in Fig. 1 are not the only ones characteristic for the surfaces of $\text{Fe}_3\text{O}_4(001)$ on $\text{Fe}(001)$. At a special tip state,²⁰ enhanced electronic contrast and resolution could be achieved with some experimental effort. Examples of such images at selected bias voltages are shown in Fig. 2. The ovals showing at the negative bias voltage ($V_s = -1.85$ V in Fig. 2a) only a minor splitting, become well resolved when the bias voltage is changed to $V_s = -0.73$ V (Fig. 2b), suggesting that they originate from two different atoms, henceforth referred to as a dimer. Moreover, the structure of rows along $\langle 110 \rangle$ spaced by 6 Å becomes very distinct. The distance between the intensity maxima in the dimers is found as 4 ± 0.1 Å, as compared with the 5.96 Å distance between the tetrahedral Fe^{3+} ions in the ideal A-layer.

The statistics of the ovals (or dimers) observed on the $\text{Fe}_3\text{O}_4(001)$ surfaces prepared on $\text{Fe}(001)$ films yields a half-monolayer of Fe(A). Therefore, we conclude that on average the surface is terminated with $\frac{1}{2}$ monolayer of Fe(A) ions, which form dimers along $\langle 110 \rangle$. The 50% occupation is realized on a large scale, whereas small areas without dimers (i.e. B terminated), with (2×2) - 12×12 Å² and with $(\sqrt{2} \times \sqrt{2})\text{R}45^\circ$ - 8.4×8.4 Å² square dimer mesh can coexist locally, as marked in Fig 1b.²¹ For surface neutrality, it is enough that the charge is compensated on the large scale by a combination of small areas with three different terminations: full A-layer, half A-layer and B-layer (presumably near defects). However, such a terminating layer, with a short-range order only, cannot be responsible for the observed $(\sqrt{2} \times \sqrt{2})\text{R}45^\circ$ reconstruction. We believe that the reconstruction comes from the outermost surface B-layer, and the arrangement of the Fe(A) dimers in the terminating layer only reflects the reconstruction.

We were also able to acquire STM images at different polarizations from the same areas for a sample prepared using the “classical” preparation method of $\text{Fe}_3\text{O}_4(001)$ on $\text{MgO}(001)$, showing in LEED also the $(\sqrt{2} \times \sqrt{2})\text{R}45^\circ$ reconstruction. It should be noted that such layers are prepared in an excess of oxygen to prevent formation of FeO . Contrary to the Fe rich surfaces, the STM images (not shown) for both polarizations are dominated by the structure of rows separated by about 6 Å. These have a typical modulation that is responsible for the $(\sqrt{2} \times \sqrt{2})\text{R}45^\circ$ reconstruction. The oval features, so characteristic for magnetite grown on the Fe buffer layer, are not visible. Clearly, our observation supports the earlier findings that such a surface is terminated with the oxygen-rich layer and the models of reconstructed B

termination apply.^{8,13}

A number of recent papers have tried to explain theoretically the structure of the (001) magnetite surface.^{22, 23, 24} In particular, Pentcheva et al. explained the $(\sqrt{2} \times \sqrt{2})R45^\circ$ reconstruction of the B-terminated surface in terms of the Jahn-Teller distortion. In present calculations the B termination reveals only minor ionic rearrangement related to the Jahn-Teller distortion while significant changes in the electronic structure of the surface are observed. The modification of the local spin moments on the surface Fe(B) gives rise to the ordering of octahedral cations: pairs of cations along the [110] direction with $\mu_{Fe(B1)}=3.50 \mu_B$ and $\mu_{Fe(B2)}=2.74 \mu_B$, are formed, similar to that discussed by Shvets et al. for the (001) surface of a bulk magnetite crystal. The changes of the magnetic moments on Fe(B) cations are related to the ordering of electrons in the $d_{x^2-y^2}$ atomic orbital. Strong interaction between oxygen *p*-band and d-electrons of Fe(B), repels the latter away from the top of the valence band into the conduction band above the Fermi level. Theoretical STM images are shown in Fig.4a,b, in which atomic positions in the bulk unit cell are shown in color for clarity. The $(\sqrt{2} \times \sqrt{2})R45^\circ$ reconstruction is clearly visible at negative bias. Two types of Fe(B) ions (represented by light and dark green, respectively) are distinguished by the different contrast of cation pairs. At positive bias, atomic rows aligned along the [110] direction image the alignment of octahedral iron on the surface. The network of regularly arranged dark features is also reproduced to some extent, whereas oval-like shapes between octahedral rows were not identified at any bias voltage. It supports our experimental conclusion that the termination of our magnetite films on the Fe (001) buffer film must be something other than the B-layer.

Due to limited computer memory, considered models of A-terminated surface were limited to selected arrangements of Fe(A) adatoms on the B-terminated surface. The termination with Fe(A) dimers is the most interesting for our STM experiments. In optimized dimer geometry the Fe(A) cations separated by $d=2.99 \text{ \AA}$ are more stable than tetrahedral irons regularly arranged on the B-layer. The dimerization originates from the electronic structure of the B-layer below and the arrangement of the outermost Fe(A) ions reflects the $(\sqrt{2} \times \sqrt{2})R45^\circ$ reconstruction. Such a termination corresponds to the highest oval density seen with STM. The theoretical STM picture of the dimeric A-surface (Fig.4c) reproduces well the experimental observation for negative sample bias. However, the full diversity of STM images for all experimental bias voltages could not be well reproduced. The reason could be a

strong on-site Coulomb interaction that further splits the occupied and empty Fe(A) states.²⁵ It is also possible that the images have been obtained with an impurity atom (eg. oxygen) attached to the tip. These effects are not included in our calculations.

According to recent DFT calculations,^{23,24} the Fe-rich termination discussed above is unstable even under oxygen-poor conditions, which remains in striking opposition to our experimental results. We note, however, that the bulk phase diagram of the FeO-Fe₂O₃ system indicates stability of magnetite for much lower oxygen partial pressure than that taken in Ref. 24 as “O-poor limit”. Moreover the random distribution of Fe(A) and dimerization on the surface is not considered in the models of Refs. 23,24.

During the decade much controversy have arisen concerning the Fe₃O₄(001) termination and reconstruction. The surface was shown to be very sensitive to preparation. Apparently conflicting STM data probably concern surfaces that are differently influenced by impurity segregation or by deviations from stoichiometry due to the reducing or oxidizing procedures applied when preparing or recovering the surface. We have proposed a new method of preparation, in which Fe₃O₄(001) films are grown on Fe(001)/Mg(001) substrates. We have shown that the surface structure of such films has a different termination than that of films grown on MgO(001) in a classical way, despite the similar reconstruction seen in low-energy electron diffraction. The analysis of the high-resolution images acquired for both negative and positive sample vs. tip polarizations leads to a consistent model of the surface, which explains and combines many features of the surface previously postulated. In particular, complexity and atomic details of the Fe(A) terminated surface, which can be obtained under Fe-rich preparation conditions, have been solved. Moreover, we have shown how the different preparation conditions – oxygen rich vs. iron rich, alter the oxide surface on the atomic scale. This opens possibilities for comparative studies of surface adsorption and reactivity.

This work was supported by the European Community under the Specific Targeted Research Project Contract No. NMP4-CT-2003-001516 (DYNASYNC). J. Korecki acknowledges the Foundation for Polish Science (FNP) for support. The authors thank Dr. N. Bailey for reading the manuscript.

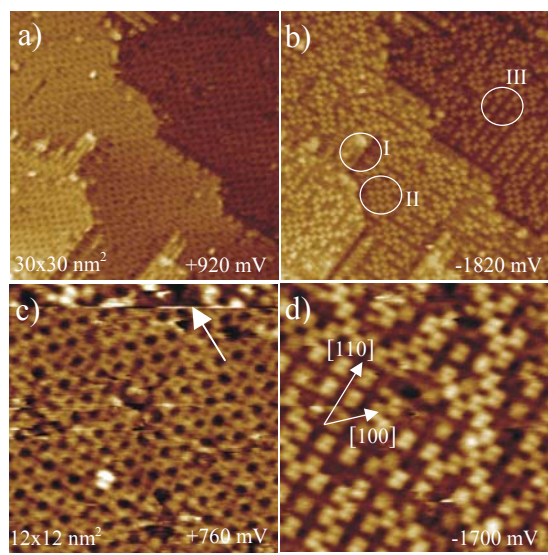


Fig.1. Constant current STM images for the $\text{Fe}_3\text{O}_4(001)$ surface of an epitaxial magnetite film on $\text{Fe}(001)/\text{MgO}(001)$. a) and b) $30 \times 30 \text{ nm}^2$ scans from the same areas taken at sample bias $V_s = 920 \text{ mV}$ and $V_s = -1820 \text{ mV}$ respectively; c), d) $12 \times 12 \text{ nm}^2$ scans from the same areas taken subsequently at sample bias $V_s = 760 \text{ mV}$ and $V_s = -1700 \text{ mV}$, respectively. The arrow in c) indicates the line where the sample bias was changed to negative. The circles in b) indicate the areas without dimers (I), with $(2 \times 2) - 12 \times 12 \text{ \AA}^2$ (II), and with $(\sqrt{2} \times \sqrt{2})\text{R}45^\circ - 8.4 \times 8.4 \text{ \AA}^2$ (III) square dimer mesh, respectively.

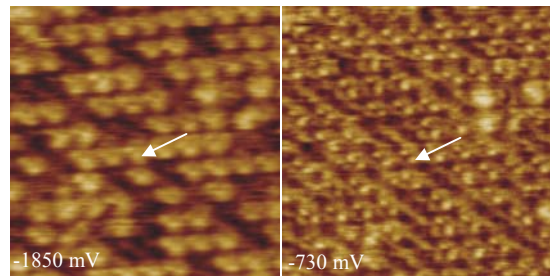


Fig.2. $12 \times 12 \text{ nm}^2$ constant current STM images for the $\text{Fe}_3\text{O}_4(001)$ surface of an epitaxial magnetite film on $\text{Fe}(001)/\text{MgO}(001)$ taken subsequently from the same area at a) -1850 mV and b) -730 mV sample bias. The arrows identify equivalent atomic positions.

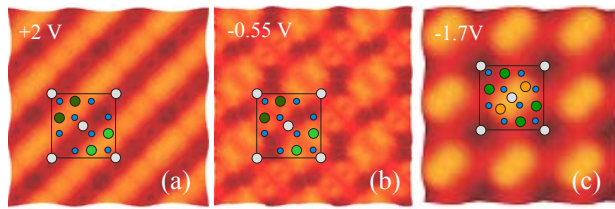


Fig.3. Theoretical STM images: a),b) B termination at negative ($V_s=-0.55$) and positive ($V_s=+2$ V) sample bias, respectively; c) dimeric A termination at positive ($V_s=+2$ V) sample bias. Circles indicate atom position in geometric $(\sqrt{2}\times\sqrt{2})R45^\circ$ surface unit cell: oxygen (blue), octahedral iron (green), surface tetrahedral iron (orange), sub-surface tetrahedral iron (white). Light and dark green colors for the octahedral sublattice are used in a) and b) to show the positions of different Fe(B) ions responsible for the $(\sqrt{2}\times\sqrt{2})R45^\circ$ reconstruction.

¹ C. Noguera, *J. Phys.: Condens. Matter* **12**, R367 (2000).

² R. Wiesendanger et al., *Science* **255** 583 (1992).

³ F. Walz, *J. Phys.: Condens. Matter* **14**, R285 (2002).

⁴ J. Garcia and G. Subias, *J. Phys.: Condens. Matter* **16**, R145 (2004).

⁵ G. Tarrach et al., *Surf. Sci.* **285**, 1 (1993).

⁶ J.M.D. Coey et al., *J. Appl. Phys.* **73**, 6742 (1993).

⁷ R. Koltun et al., *Appl. Phys. A* **73**, 49 (2001).

⁸ G. Mariotto, S. Murphy, I. V. Shvets, *Phys. Rev. B* **66**, 245426 (2002).

⁹ J.M. Gaines et al., *Surf. Sci.* **373**, 85 (1997). J.M. Gaines et al., *Mater. Res. Soc. Symp. Proc. Vol. 474*, 191 (1997).

¹⁰ F.C. Voogt, Ph.D. Thesis, Departments of Chemical Physics and Nuclear Solid State Physics, University of Groningen, Netherlands, 1998. F.C. Voogt et al., *Phys. Rev. B* **60**, 11193 (1999).

¹¹ S.A. Chambers, S.A. Joyce, *Surf. Sci.* **420**, 111 (1999).

¹² S.A. Chambers, S. Thevuthasan, S.A. Joyce, *Surf. Sci.* **450**, L273 (2000).

¹³ B. Stanka et al., *Surf. Sci.* **448**, 49 (2000).

¹⁴ A.V. Mijiritskii, D.O. Boerma, *Surf. Sci.* **486**, 73 (2001).

¹⁵ N. Spiridis et al., *J. Phys. Chem. B* **108**, 14356 (2004).

¹⁶ J. Korecki, et al., *Thin Solid* **412**, 14 (2002).

¹⁷ <http://www.fysik.dtu.dk/campos/Dacapo/>

¹⁸ J. P. Perdew, et al., *Phys. Rev. B* **46** 6671 (1992).

¹⁹ J. Tersoff and D.R. Hamann, *Phys. Rev. Lett.* **50** 1998 (1983).

²⁰ M. Schmid, H. Stadler, and P. Varga, *Phys. Rev. Lett.* **70**, 1441 (1993)

²¹ The small areas with (2x2) reconstruction give rise to weak and broad LEED spots visible at the electron energy as low as 20 eV.

²² I. V. Shvets, et al., *Phys. Rev. B* **70**, 155406 (2004)

²³ C. Cheng, *Phys. Rev. B* **71**, 052401 (2005)

²⁴ R. Pentcheva et al., *Phys. Rev. Lett.* **94**, 126101 (2005).

²⁵ H.-T. Jeng, G. Y. Guo, and D. J. Huang, *Phys. Rev. Lett.* **93**, 156403 (2004).